

## Time dependence of the vacuum-uv emissions from neon, and energy transfers to the resonance states $\text{Ne}(^1P_1)$ and $\text{Ne}(^3P_1)$ in helium-neon mixtures

Peter K. Leichner, J. D. Cook, and Stephen J. Luerman

*Department of Physics and Astronomy, University of Kentucky, Lexington, Kentucky 40506*

(Received 2 June 1975)

Time-resolved studies of the vacuum-uv emissions from neon and helium-neon mixtures were made using a single-photon counting technique. Excitation of the atoms was provided by a pulsed beam of 250-keV electrons. Measurements in neon were carried out at the wavelengths of the resonance states  $\text{Ne}(^1P_1)$  and  $\text{Ne}(^3P_1)$ . Collision coefficients for the destruction of  $\text{Ne}(^1P_1)$ ,  $\text{Ne}(^3P_1)$ , and  $\text{Ne}(^3P_2)$  atoms in neon were determined. The two-body collision coefficient for deexcitation of  $\text{Ne}(^1P_1)$  atoms to the  $\text{Ne}(^3P_1)$  state is  $5.5 \times 10^4 \text{ sec}^{-1}/\text{Torr}$ . Atoms in the  $\text{Ne}(^3P_1)$  level undergo two- and three-body collisions with neon ground-state atoms. The deexcitation rate for the transition  $\text{Ne}(^3P_1)$  to  $\text{Ne}(^3P_2)$  is  $1.80 \times 10^3 \text{ sec}^{-1}/\text{Torr}$ . The three-body collision coefficient for  $\text{Ne}(^3P_1)$  is  $5.0 \text{ sec}^{-1}/\text{Torr}^2$ . Metastable  $\text{Ne}(^3P_2)$  atoms are collisionally excited to the  $\text{Ne}(^3P_1)$  state at the rate  $160 \text{ sec}^{-1}/\text{Torr}$ , and they are destroyed in three-body collisions with rate coefficient  $0.60 \text{ sec}^{-1}/\text{Torr}^2$ . The two-body deexcitation frequency for  $\text{Ne}(^3P_1)$  and two- and three-body collision coefficients for  $\text{Ne}(^3P_2)$  are in agreement with the results of Phelps. Studies of the emissions from He-Ne mixtures were performed at relatively high helium pressures of 200 and 400 Torr, respectively. At each helium pressure controlled amounts of neon impurity were added. Time-resolved measurements were made at the wavelengths of the  $\text{He}(2^1S)$  metastable, the helium continuum emissions, and at the wavelengths of  $\text{Ne}(^1P_1)$  and  $\text{Ne}(^3P_1)$ . The decay constants for  $\text{He}(2^1S)$  and  $\text{Ne}(^1P_1)$  are shown to be consistent with resonant excitation transfer from  $\text{He}(2^1S)$  to the  $\text{Ne}(3s_2)$  laser level (Paschen notation). The pressure dependence of the emissions from  $\text{Ne}(^3P_1)$  in helium is governed primarily by collisional deexcitation to the metastable  $\text{Ne}(^3P_2)$  state. The two-body collision coefficient for the destruction of  $\text{Ne}(^3P_1)$  atoms by helium is  $8.3 \times 10^3 \text{ sec}^{-1}/\text{Torr}$ .

### I. INTRODUCTION

Time-resolved spectroscopic studies of the emissions from noble gases excited with energetic charged particles have provided much new information about the excitation and relaxation of atomic and molecular species. The ability to rapidly inject energy into gases over wide pressure ranges makes it possible to determine collision coefficients and molecular lifetimes that would be difficult to obtain from other types of experiments or from theory. Much of the current interest in vacuum-uv emissions from noble gases has arisen because of laser applications.<sup>1</sup> Detailed knowledge of atomic collision rates and of excimer formation and decay is essential for an understanding of the mechanisms which lead to stimulated emission in high-pressure noble gases.<sup>2</sup>

The objective of the present paper is twofold. We report new experimental results for the pressure dependence of the emissions from  $\text{Ne}(^1P_1)$  and  $\text{Ne}(^3P_1)$  in neon. Secondly, we have studied energy transfers to the same resonance states in He-Ne mixtures. For pure neon, we have extended the emission study of Leichner<sup>3</sup> to lower pressures to obtain additional information about collision coefficients for the lowest excited states. The im-

portance of low-pressure data is that they reveal atomic features which cannot be observed at higher pressures. In particular,  $\text{Ne}(^1P_1)$  atoms are rapidly depleted in two-body collisions with neon ground-state atoms. At pressures of a few Torr, this collision frequency exceeds the rate of escape of imprisoned resonance radiation. Consequently, the investigation of emissions from  $\text{Ne}(^1P_1)$  is limited to relatively low gas pressures.

Low-pressure data for the emissions from neon at the 744-Å resonance line are combined with previous results<sup>3</sup> to obtain pressure-dependent lifetimes of  $\text{Ne}(^3P_1)$  and  $\text{Ne}(^3P_2)$  atoms in the range from 4 to 1000 Torr. Emissions from the  $\text{Ne}(^3P_1)$  level give information about both the  $\text{Ne}(^3P_1)$  and  $\text{Ne}(^3P_2)$  states because of collisional excitation of the metastable to the nearest radiating state. The two-body destruction rate for  $\text{Ne}(^3P_1)$  atoms and two- and three-body collision coefficients for  $\text{Ne}(^3P_2)$  are in good agreement with the absorption study of Phelps.<sup>4</sup> In addition, we have determined the two-body deexcitation frequency for  $\text{Ne}(^1P_1)$  atoms and the three-body collision coefficient for  $\text{Ne}(^3P_1)$ . These could not be measured by the absorption technique. Based on time-resolved data and on the theoretical work of Cohen and Schneider,<sup>5,6</sup> we argue that the large two-body coefficient

for  $\text{Ne}(^1P_1)$  represents collisional deexcitation to the  $\text{Ne}(^3P_1)$  state. Furthermore, we construct a kinetic model for the formation of excited neon molecules. This model is consistent with experimentally observed features and with theory.

To examine energy-transfer reactions in He-Ne mixtures, we have measured the time dependence of the vacuum-uv emissions from the  $\text{He}(2^1S)$  metastable, from the  $\text{He}(A^1\Sigma_u^+)$  molecule, and from the resonance states  $\text{Ne}(^1P_1)$  and  $\text{Ne}(^3P_1)$ . This investigation differs from earlier measurements<sup>8-15</sup> in several aspects. The helium host gas is at relatively high pressures of 200 and 400 Torr, respectively, with neon partial pressures ranging from 0.05 to 5 Torr. At these high helium pressures, collision processes compete with and even dominate radiative transitions. Furthermore, we present time-resolved measurements for excitation transfer from the helium host gas to the lowest excited states of neon. These data are shown to be consistent with gas-discharge results<sup>12</sup> in that the initial excitation transfer appears to be primarily to the  $\text{Ne}(3s_2)$  laser level. Atoms in the  $\text{Ne}(3s_2)$  state are subsequently destroyed by radiative transitions and by two-body collisions with helium ground-state atoms. For the helium pressures used in this experiment, collisional destruction of  $\text{Ne}(3s_2)$  atoms is several decades faster than the radiative transition rate. In particular, the large reverse resonant-transfer rate from  $\text{Ne}(3s_2)$  to  $\text{He}(2^1S)$  causes most of the excitation energy to be returned to the helium metastable. Therefore, energy is rapidly transferred in the forward and reverse directions between  $\text{He}(2^1S)$  and  $\text{Ne}(3s_2)$ . Under these conditions the net destruction rate of  $\text{He}(2^1S)$  is governed by the rate at which excitation can be collisionally transferred from  $\text{Ne}(3s_2)$  to other upper levels of the neon atom. The lowest excited states of neon are primarily populated by cascading from these upper levels. We show that the measured time dependence of the emissions from  $\text{He}(2^1S)$  and  $\text{Ne}(^1P_1)$  atoms can be explained in terms of the transfer processes outlined above. The final decay of  $\text{Ne}(^3P_1)$  atoms in helium is governed primarily by collisional deexcitation to the  $\text{Ne}(^3P_2)$  metastable.

## II. EXPERIMENTAL METHOD

The experimental apparatus and technique are similar to those used previously in an emission study of neon.<sup>3</sup> For completeness we give a brief description. A pulsed beam of 250-keV electrons produces a narrow pencil of excited atoms along the axis of a cylindrical stainless-steel emission cell. The cell has a radius of 2 cm and a length of 16 cm. Electron pulse widths are continuously

variable from 50 nsec to 12  $\mu\text{sec}$ , with repetition rates ranging from 2 to 20 kHz. Typical electron currents used in this experiment ranged from about 0.01 to about 0.1  $\mu\text{A}$ , with excitation pulse widths ranging from 0.1 to 3  $\mu\text{sec}$ . No dependence of the time-dependent emissions on either current or pulse width was observed.

Photons emitted by the excited gas enter a vacuum-uv scanning monochromator, are dispersed by a diffraction grating, and are detected with a single-photon detector. Time-resolved measurements are carried out using a time-of-flight technique. Since the helium and neon emissions from the lowest excited states occur below 1000  $\text{\AA}$ , the gas is differentially pumped to keep the monochromator evacuated. Helium gas used was Matheson research grade with the following impurities (in ppm):  $\text{O}_2 < 1$ ,  $\text{N}_2 < 5$ , and  $\text{CH}_4 < 0.5$ . Neon gas used with Linde ultrahigh purity with an assayed purity of 99.995%. Total and partial pressures were measured with an MKS Baratron gauge. Experimental errors are estimated at 10% in absolute magnitude and at 5% in relative magnitude.

## III. NEON RESULTS

In this section we report new experimental results for the time dependence of the emissions from neon at the wavelengths of the resonance states  $\text{Ne}(^1P_1)$  and  $\text{Ne}(^3P_1)$ . Measurements were made at relatively low gas pressures up to 35 Torr. Figure 1 shows typical low-pressure emission spectra. The emission intensity at 744  $\text{\AA}$  increases rapidly with increasing pressure, whereas the intensity at 736  $\text{\AA}$  does not. At pressures slightly higher than those shown in Fig. 1, the intensity at 736  $\text{\AA}$  decreases with increasing pressure. At about 40 Torr the emissions at this wavelength are too weak to make time-resolved measurements.

Typical time-resolved spectra for the two resonance lines at a pressure of 8 Torr are shown in Fig. 2. Emissions at the 736- $\text{\AA}$  ( $^1P_1$ ) line are characterized by a fast decay corresponding to a single exponential term. The emissions from  $\text{Ne}(^3P_1)$  at 744  $\text{\AA}$  exhibit a rapid initial buildup in intensity and a subsequent decay which extends over about 200  $\mu\text{sec}$ . This buildup occurs within the 6- $\mu\text{sec}$  decay time of the  $\text{Ne}(^1P_1)$  atoms. The decay of  $\text{Ne}(^3P_1)$  photons is characterized by the sum of two exponential terms. An analysis of the time evolution of the emissions from the two resonance states is given below.

### A. $\text{Ne}(^1P_1)$ Analysis

In Fig. 3 we have plotted the  $\text{Ne}(^1P_1)$  decay constant in the pressure range from 1 to 35 Torr.

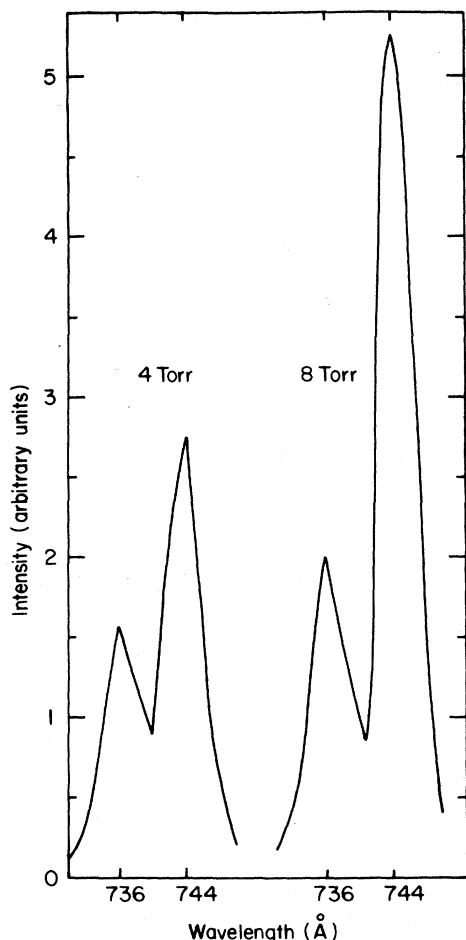


FIG. 1. Low-pressure neon emission spectra at the 736-Å ( $^1P_1$ ) and 744-Å ( $^3P_1$ ) resonance lines.

The solid line was obtained by a least-squares analysis. A pressure-independent term and a two-body collision term were required to fit the data. There is no evidence of three-body collisions in this pressure range. The  $\text{Ne}(^1P_1)$  decay

constant may therefore be written as

$$u(^1P_1) = \beta_1 + k_1 P_{\text{Ne}}, \quad (1)$$

where  $P_{\text{Ne}}$  is the neon pressure in Torr, and where

$$\beta_1 = 2.6 \times 10^5 \text{ sec}^{-1}, \quad (2)$$

$$k_1 = 5.5 \times 10^4 \text{ sec}^{-1}/\text{Torr}, \quad (3)$$

so that  $u(^1P_1)$  is in units of  $\text{sec}^{-1}$ . The constant  $\beta_1$  is somewhat larger than but not inconsistent with the imprisonment decay constant calculated from Holstein's theory<sup>16</sup> according to the relation

$$\beta = (0.207/\tau)(\lambda/R)^{1/2}, \quad (4)$$

where  $\tau$  is the natural lifetime of the radiating state,  $\lambda$  is the corresponding wavelength, and  $R$  is the radius of the emission cell. Using the lifetime measurements of Lawrence and Liszt,<sup>17</sup> we find a theoretical value of  $2.2 \times 10^5 \text{ sec}^{-1}$  for  $\beta_1$ . The larger experimental value may arise from systematic errors in determining a pressure-independent decay constant. However, the recent calculations of Payne *et al.*<sup>18</sup> show that at low pressures (of the order of a few Torr and below) the assumption of complete redistribution in frequency of the resonance radiation is no longer satisfied. Deviation from Holstein's theory may therefore be expected.

Of particular interest is the large two-body collision coefficient  $k_1$  for the destruction of  $\text{Ne}(^1P_1)$  atoms in collisions with neon ground-state atoms. Since the lowest excited states of neon are closely spaced in energy, an appreciable fraction of ground-state atoms can cause transitions between excited levels. Collisional deexcitation of metastables and resonance atoms to the ground state is assumed negligible because of the large conversion of potential energy to kinetic energy required. The level closest to  $\text{Ne}(^1P_1)$  is the metastable state  $\text{Ne}(^3P_0)$ . From energy considerations, one would

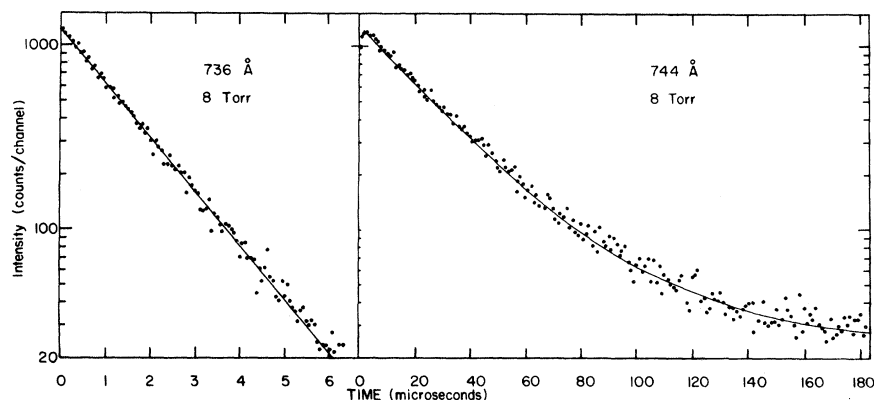


FIG. 2. Typical low-pressure time-resolved spectra for the  $\text{Ne}(^1P_1)$  and  $\text{Ne}(^3P_1)$  resonance states.

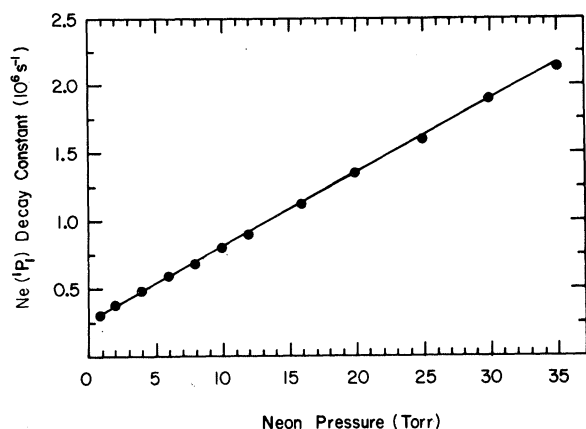


FIG. 3. Pressure dependence of the emissions from  $\text{Ne}(^1P_1)$ .

therefore expect that  $\text{Ne}(^1P_1)$  atoms are primarily deexcited to the upper metastable state. However, in view of the time-resolved spectra (Fig. 2) and because of potential-energy curves<sup>5</sup> now available, we believe that the dominant relaxation mechanism for the  $\text{Ne}(^1P_1)$  level is collisional deexcitation to the lowest resonance state  $\text{Ne}(^3P_1)$ .

The calculations of Cohen and Schneider<sup>5</sup> show that spin-orbit coupling effects of  $\text{Ne}_2$  molecular states lead to several avoided crossings. Crossing is avoided by the pairs  $0_g^-(^3P_2)$ ,  $0_g^-(^3P_0)$  and  $1_g(^3P_2)$ ,  $1_g(^3P_1)$  and  $0_g^+(^3P_1)$ ,  $0_g^+(^1P_1)$ . The latter of these implies that the  $\text{Ne}(^1P_1)$  and  $\text{Ne}(^3P_1)$  states are strongly coupled, which makes rapid transfer of excitation energy possible. We therefore conclude that at low pressures the decay of  $\text{Ne}(^1P_1)$  atoms is governed primarily by the escape of resonance radiation from the emission cell and by collisional deexcitation to the  $\text{Ne}(^3P_1)$  resonance state.

#### B. $\text{Ne}(^3P_1)$ and $\text{Ne}(^3P_2)$ analysis

We turn now to an analysis of the time-resolved spectra at the  $744\text{-}\text{\AA}$  ( $^3P_1$ ) resonance line. It is evident from Fig. 2 that the  $\text{Ne}(^1P_1)$  state plays no role in the final decay of the emissions from  $\text{Ne}(^3P_1)$ . This is in agreement with the observations of Phelps,<sup>4</sup> who found no measurable  $\text{Ne}(^1P_1)$  density during the afterglow. In the analysis presented below we therefore assume that the final decay of  $\text{Ne}(^3P_1)$  atoms is decoupled from the  $\text{Ne}(^1P_1)$  level.

As shown below, the two decay components (fast and slow) of the emissions at  $744\text{ \AA}$  need to be analyzed in terms of two coupled differential equations involving the  $\text{Ne}(^3P_2)$  levels. Figure 4 shows the pressure dependence of the fast-decay component. A pressure-independent term and

two- and three-body collision terms are evident. The pressure-independent constant is characteristic of trapped resonance radiation from the  $\text{Ne}(^3P_1)$  level. The solid line in Fig. 4 represents the equation

$$r_1 = 1.86 \times 10^4 + 1.80 \times 10^3 P_{\text{Ne}} + 5.18 P_{\text{Ne}}^2, \quad (5)$$

where  $r_1$  is in units of  $\text{sec}^{-1}$ . The pressure dependence of the slow-decay component is displayed in Fig. 5. The solid line is given by

$$r_2 = 160 P_{\text{Ne}} + 0.40 P_{\text{Ne}}^2, \quad (6)$$

also in units of  $\text{sec}^{-1}$ . Note that in Figs. 4 and 5, low-pressure data from 4 to 30 Torr represent new measurements. Data from 50 to 1000 Torr are based on results previously obtained by Leichner.<sup>3</sup>

The analysis of the various terms in Eqs. (5) and (6) is facilitated by the following observation: The two-body term in Eq. (5) is in good agreement with the deexcitation frequency from  $\text{Ne}(^3P_1)$  to  $\text{Ne}(^3P_2)$  determined by Phelps in an absorption study. The three-body term which suggests the formation of excited neon molecules could not be measured by the absorption technique. In Eq. (6), the two- and three-body collision coefficients are also comparable to values obtained by Phelps. The two-body term in this equation represents collision-induced excitation from  $\text{Ne}(^3P_2)$  to  $\text{Ne}(^3P_1)$ . The three-body coefficient gives rise to excited neon molecules. Because of the collisional excitation transfer between the  $\text{Ne}(^3P_1)$  and  $\text{Ne}(^3P_2)$  levels, the emissions observed at  $744\text{ \AA}$

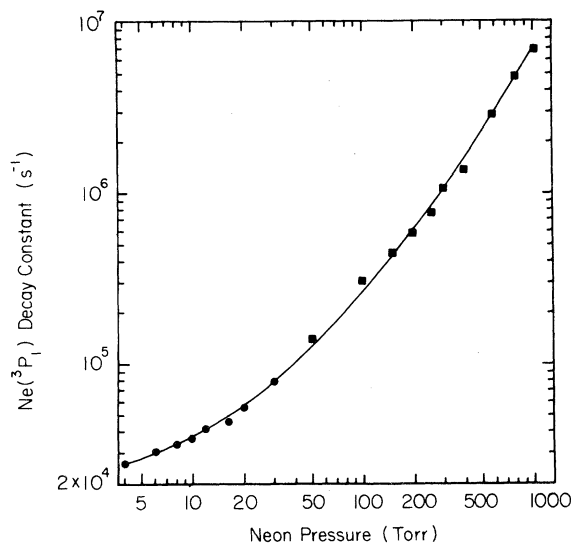


FIG. 4. Pressure dependence of the fast-decay component of the emissions from  $\text{Ne}(^3P_1)$ . Points shown by circles represent new measurements. Data points indicated by squares are from Ref. 3.

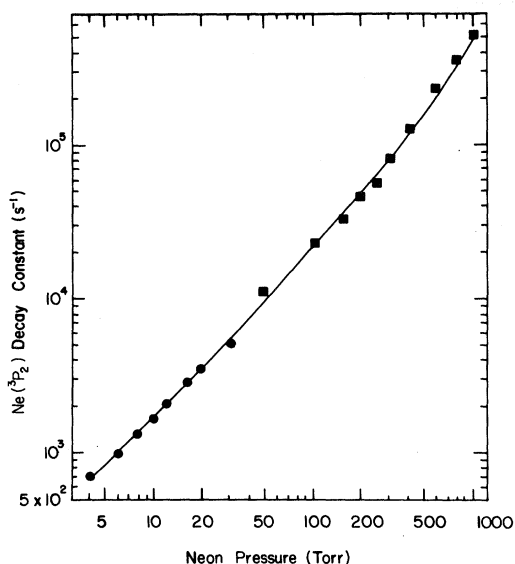


FIG. 5. Pressure dependence of the slow-decay component of the emissions from  $\text{Ne}(^3P_1)$ . Circles represent new measurements. Squares are from Ref. 3.

have as their origin both atomic states. The fast-decay component represents primarily the destruction of  $\text{Ne}(^3P_1)$  atoms, and the slow-decay component is due to the destruction of  $\text{Ne}(^3P_2)$  atoms. To separate the decay components and to obtain more reliable collision coefficients than those given by Eqs. (5) and (6), we analyze the data in terms of the differential equations which govern the decay of the two lowest excited states of neon.

The above statements are summarized in Fig. 6. Atoms in the  $\text{Ne}(^3P_1)$  state decay by the emission of resonance radiation, by deexcitation to  $\text{Ne}(^3P_2)$ , and in three-body collisions which lead to the formation of  $\text{Ne}_2 0_u^+(^3P_1)$  molecules. The  $\text{Ne}(^3P_2)$  level is depleted by excitation to  $\text{Ne}(^3P_1)$  and by three-

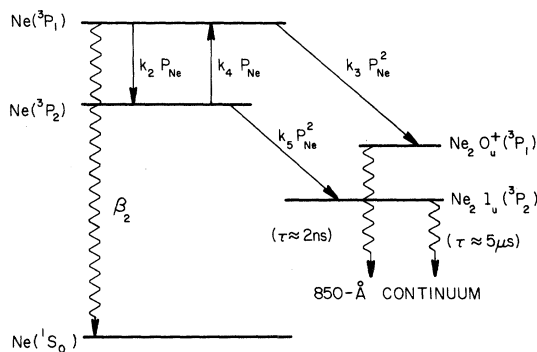


FIG. 6. Rate diagram for the decay of  $\text{Ne}(^3P_1)$  and  $\text{Ne}(^3P_2)$  atoms.

body collisions which give rise to  $\text{Ne}_2 1_u(^3P_2)$  molecules. The identification of the molecular levels is based on the work of Cohen and Schneider, as is the lifetime of the  $\text{Ne}_2 0_u^+(^3P_1)$  molecule. The 5- $\mu\text{sec}$  lifetime of the  $\text{Ne}_2 1_u(^3P_2)$  level represents a pressure-independent lifetime measured by Leichner, in agreement with a mean lifetime expected from theory.<sup>6</sup>

The differential equations governing the excited-state populations of the atomic levels may be written as

$$\frac{dR_1}{dt} = -(\beta_2 + k_2 P_{\text{Ne}} + k_3 P_{\text{Ne}}^2) R_1 + k_4 P_{\text{Ne}} M_1, \quad (7)$$

$$\frac{dM_1}{dt} = k_2 P_{\text{Ne}} R_1 - (k_4 P_{\text{Ne}} + k_5 P_{\text{Ne}}^2) M_1, \quad (8)$$

where  $R_1$  and  $M_1$  denote the number of atoms in the resonance and metastable states, respectively. In the above equations, we have assumed that inverse processes corresponding to upward transitions from excited molecular levels to excited atomic states are negligibly small. The assumption appears justified, because in neon the molecular continuum occurs at about 850 Å and is well separated from excited atomic states. Furthermore, the molecular lifetimes are relatively short, and the depth and shape of the potential wells<sup>5</sup> suggest that neon molecules are primarily deexcited by transitions to the repulsive ground state which promptly dissociates.

With this assumption, Eqs. (7) and (8) may be solved to yield

$$R_1(t) = A_1 e^{-r_1 t} + A_2 e^{-r_2 t}, \quad (9)$$

where  $A_1$  and  $A_2$  are constants, and where  $r_1$  and  $r_2$  are given by Eqs. (5) and (6). In Appendix A it is shown that the unknown collision coefficients  $k_2$  to  $k_5$  can be evaluated in terms of the two measured quantities  $r_1$  and  $r_2$ . From the results in Appendix A it follows that the  $\text{Ne}(^3P_1)$  decay constant is given by

$$u(^3P_1) = \beta_2 + k_2 P_{\text{Ne}} + k_3 P_{\text{Ne}}^2, \quad (10)$$

with

$$\beta_2 = 1.9 \times 10^4 \text{ sec}^{-1}, \quad (11)$$

$$k_2 = 1.8 \times 10^3 \text{ sec}^{-1}/\text{Torr}, \quad (12)$$

$$k_3 = 5.0 \text{ sec}^{-1}/\text{Torr}^2. \quad (13)$$

For the  $\text{Ne}(^3P_2)$  metastable we find

$$u(^3P_2) = k_4 P_{\text{Ne}} + k_5 P_{\text{Ne}}^2, \quad (14)$$

where

$$k_4 = 160 \text{ sec}^{-1}/\text{Torr}, \quad (15)$$

$$k_5 = 0.60 \text{ sec}^{-1}/\text{Torr}^2. \quad (16)$$

The coefficients  $k_2$ ,  $k_4$ , and  $k_5$  are in good agreement with the results of Phelps. As mentioned previously, the three-body collision coefficient  $k_3$  could not be measured by the absorption technique. As in the case of  $\text{Ne}(^1P_1)$ , the pressure-independent decay constant  $\beta_2$  is larger than what is obtained from Holstein's theory. Using Eq. (4), we find a theoretical value of  $1.3 \times 10^4 \text{ sec}^{-1}$ . We note in this connection that Phelps also found that experiment yields a larger value than theory.

The analysis of the lowest excited states of neon has not included the  $\text{Ne}(^3P_0)$  level. We believe that this is justified for the following reasons. The initial excitation of neon by 250-keV electrons probably satisfies the optical approximation, so that the amount of energy transferred to a particular excited state is proportional to the oscillator strength of this state. Consequently, the resonance states  $\text{Ne}(^1P_1)$  and  $\text{Ne}(^3P_1)$  should be richly populated by the incident beam pulse. Of course, low-energy secondary electrons will also excite atomic states, and these excitations will not satisfy the optical approximation. Nevertheless, experimental evidence suggests that when high-energy electrons or protons interact with noble gases and when low excitation currents are used, it is primarily the resonance states which are excited. Therefore, the  $\text{Ne}(^3P_0)$  population in the experiment reported here was probably too low to have an effect on time-resolved measurements. Furthermore, the  $\text{Ne}(^3P_0)$  potential energy curves<sup>5</sup> are repulsive at nearly all internuclear separations, so that excitation transfer from  $\text{Ne}(^1P_1)$  or  $\text{Ne}(^3P_1)$  to the upper metastable should be negligible. On the other hand, the potential energy curves for the  $\text{Ne}(^3P_2)$  level exhibit an attractive potential well and the previously mentioned avoided crossing  $1_g(^3P_2)$ ,  $1_g(^3P_1)$ . Consequently, one may expect the lowest metastable to be populated by deexcitation of  $\text{Ne}(^3P_1)$  atoms. This is precisely what is observed.

### C. 850-Å continuum radiation

We comment briefly on time-resolved measurements at the wavelength of the 850-Å continuum reported in a previous publication.<sup>3</sup> It was found that the intensity of the molecular emissions continued to increase for a relatively long time after the excitation pulse had passed through the gas. The time delay in reaching peak intensity ranged from about 20  $\mu\text{sec}$  at 100 Torr of neon pressure to about 2  $\mu\text{sec}$  at 1000 Torr. From the rise time of the continuum emissions it was calculated<sup>3</sup> that excited molecules are created in three-body collisions at the rate  $0.6P_{\text{Ne}}^2$ . A pressure-independent molecular lifetime of about 5  $\mu\text{sec}$  was established.

These experimental results can be explained in terms of the processes indicated in Fig. 6. The measured lifetime corresponds to radiative transitions from vibrational levels of the  $\text{Ne}_2 1_u(^3P_2)$  molecule to the repulsive ground state. This molecule is created at a rate equal to the rate at which  $\text{Ne}(^3P_2)$  atoms are destroyed in three-body collisions—namely,  $0.60P_{\text{Ne}}^2$ . Time-resolved measurements at the wavelengths of the atomic and the molecular emissions are therefore in excellent agreement. We point out, however, that the new experimental and theoretical results no longer support the existence of a metastable neon molecule suggested in Ref. 3.

## IV. HELIUM-NEON RESULTS

In this section we examine energy transfers to the resonance states  $\text{Ne}(^1P_1)$  and  $\text{Ne}(^3P_1)$  in He-Ne mixtures. Measurements of the pressure dependence of the lifetimes of  $\text{He}(2^1S)$ ,  $\text{Ne}(^1P_1)$  and  $\text{Ne}(^3P_1)$  were made at relatively high helium pressures of 200 and 400 Torr, respectively. At each helium pressure, controlled amounts of neon impurity were added. Decay constants were determined as a function of neon partial pressure in the high-pressure helium host gas.

Because of the complexity of the collision processes which take place in gas mixtures at pressures of a few hundred Torr, an understanding of the emissions from pure helium is essential for the interpretation of time-resolved measurements in He-Ne mixtures. The vacuum-uv emissions from pure helium have been investigated experimentally in detail by Bartell *et al.*<sup>7</sup> Furthermore, Payne *et al.*<sup>19</sup> have recently examined the kinetic processes which determine the time dependence of the vacuum-uv emissions from helium. These authors have shown that most of the large  $\text{He}(2^1P)$  population generated by the incident charged particles is converted rapidly to the  $\text{He}(2^1S)$  metastable state either by radiative transition, by two-body collision processes, or by the related predissociation of the  $B^1\Pi_g$  molecule. The collision coefficients<sup>7,19</sup> are large, so that at pressures of a few hundred Torr the  $\text{He}(2^1P)$  population is small whereas the  $\text{He}(2^1S)$  level is richly populated.

Helium emission spectra at 200 and 400 Torr are shown in Fig. 7. These spectra are characterized by a fairly sharp peak at the 601-Å  $\text{He}(2^1S)$  line, and by continuum emissions extending to about 1000 Å. As explained in the last paragraph, at these helium pressures emissions from  $\text{He}(2^1P)$  are too weak to be observed. The pressure dependence of the  $\text{He}(2^1S)$  decay constant is given by<sup>19</sup>

$$u(2^1S) \approx 150P_{\text{He}} + 1.3P_{\text{He}}^2, \quad (17)$$

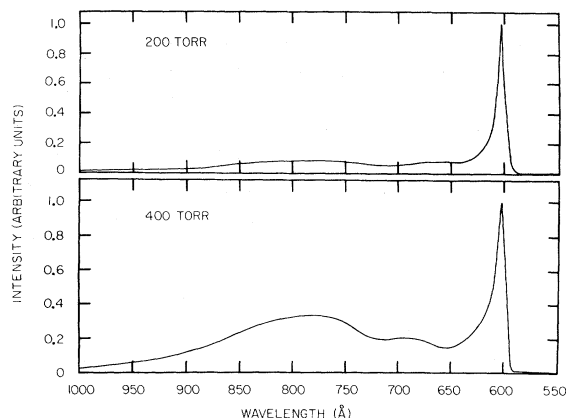


FIG. 7. Helium emission spectra as a function of pressure and wavelength.

in units of  $\text{sec}^{-1}$ . The linear term represents collision-induced radiation from  $\text{He}(2^1\text{S})$ . The three-body term represents the formation of  $\text{He}_2(A^1\Sigma_u^+)$  which radiates to the repulsive ground state and dissociates. The light emitted in this transition would be expected to have the same time dependence as the 601-Å radiation at pressures such that the decay of  $\text{He}(2^1\text{S})$  does not approach the transition rate of the  $A^1\Sigma_u^+$  molecule. For pressures up to 1000 Torr, Bartell *et al.* have observed that the emissions in the wavelength region  $601 \leq \lambda \leq 950 \text{ \AA}$  have the decay rate given by Eq. (17). Therefore, destruction of  $\text{He}(2^1\text{S})$  is the rate-limiting step for molecular emissions in this pressure range. The implication is that the  $A^1\Sigma_u^+$  molecule has a relatively short lifetime and is therefore not a likely energy donor in He-Ne

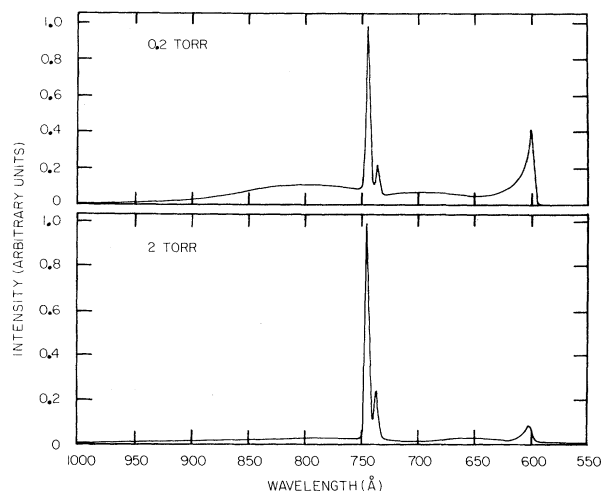


FIG. 8. Emission spectra from He-Ne mixtures at a constant helium pressure of 400 Torr. Neon partial pressures are 0.2 and 2 Torr, as indicated in the figure.

mixtures. On the other hand, the decay rate of  $\text{He}(2^1\text{S})$  is very much lower than that of any other singlet state, so that it is strongly affected by impurities. The experimental data presented below show that even at relatively high helium pressures the energy-transfer reactions in He-Ne mixtures can be explained in terms of resonant energy transfer from  $\text{He}(2^1\text{S})$  to  $\text{Ne}(3s_2)$ . Molecule-atom energy transfers which have been reported for the heavier rare gases<sup>20</sup> evidently play no role in He-Ne excitation transfers.

Having examined the time dependence of the vacuum-uv emissions from neon and helium, we are now in a position to analyze the emissions from He-Ne mixtures. In Fig. 8, time-unresolved emission spectra are shown at a helium pressure of 400 Torr and neon partial pressures of 0.2 and 2 Torr, respectively. Quenching of the emissions from  $\text{He}(2^1\text{S})$  as a function of neon partial pressure is evident. Both spectra are dominated by intense emissions from the  $\text{Ne}(^3P_1)$  level. The intensity at the wavelength of the  $\text{Ne}(^1P_1)$  state is much lower at all neon partial pressures. Furthermore, the intensity of the radiation from the resonance states of neon in He-Ne mixtures greatly exceeds the intensity of the emissions from pure neon at comparable neon pressures. Direct excitation of  $\text{Ne}(^1P_1)$  and  $\text{Ne}(^3P_1)$  by the electron beam was determined to be negligible in comparison with excitation transfer from  $\text{He}(2^1\text{S})$  to neon.

Figure 9 summarizes time-resolved measurements as a function of neon partial pressure at the wavelength of the  $\text{He}(2^1\text{S})$  metastable. Measurements for identical helium pressures and neon impurities were also made at the maxima of the helium continuum emissions at 675 and 825 Å. Within experimental error, the decay constants at the latter wavelengths are the same as those at 601 Å. Extrapolation to zero neon partial pressure yields excellent agreement at all wavelengths with the results of Bartell *et al.* for pure helium.<sup>7</sup> We conclude that in helium and in He-Ne mixtures the destruction of the  $\text{He}(2^1\text{S})$  metastable is the rate-limiting step for the decay of the  $\text{He}_2(A^1\Sigma_u^+)$  molecule. The solid lines in Fig. 9 represent the equation

$$\gamma(2^1\text{S}) = 4.1 \times 10^5 P_{\text{Ne}}, \quad (18)$$

in units of  $\text{sec}^{-1}$ . This is the net destruction rate of  $\text{He}(2^1\text{S})$  atoms resulting from collisions with neon ground-state atoms. Within experimental error it is the same for helium host-gas pressures of 200 and 400 Torr. It is shown below that the two-body coefficient given by Eq. (18) is consistent with the cross-section measurements of Benton *et al.*<sup>9</sup> and with other data for excitation transfer in the He-Ne system.

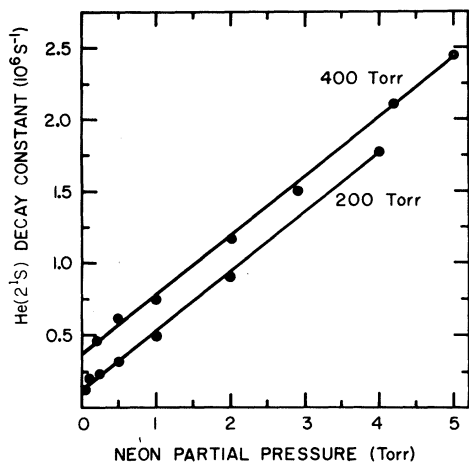


FIG. 9. He( $2^1S$ ) decay constant at helium pressures of 200 and 400 Torr as a function of neon partial pressure.

Typical time-resolved spectra for Ne( $^1P_1$ ) and Ne( $^3P_1$ ) in He-Ne mixtures are displayed in Fig. 10. There are several features which distinguish these spectra from the pure neon spectra given in Fig. 2. The Ne( $^1P_1$ ) decay at 736 Å is now characterized by the sum of two exponential terms. The second (slow) component has a small amplitude, and is observed only for low neon impurity concentration. It is probably due to emissions from the helium molecule at the same wavelength, and we have not included it in the subsequent analysis of the Ne( $^1P_1$ ) decay constant. The time evolution of the Ne( $^3P_1$ ) emissions at 744 Å shows a buildup in intensity at early times and a decay at later times that is characterized by a single exponent. The initial buildup arises from collisional deexcitation of Ne( $^1P_1$ ) to Ne( $^3P_1$ ) and probably from conversion of metastable states to the lowest radiating state. The final decay of Ne( $^3P_1$ ) persists long after the emissions from Ne( $^1P_1$ ) and from helium have ceased. It represents primarily the collisional deexcitation of Ne( $^3P_1$ ) to Ne( $^3P_2$ ).

In Figs. 11 and 12 we have plotted the Ne( $^1P_1$ ) and Ne( $^3P_1$ ) decay constants as a function of neon

partial pressure. Within experimental error, these decay constants are identical at helium pressures of 200 and 400 Torr. The solid lines in Figs. 11 and 12 are respectively given by

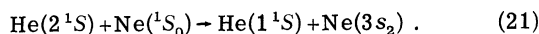
$$\gamma(^1P_1) = 1.1 \times 10^5 P_{\text{Ne}} \quad (19)$$

for the Ne( $^1P_1$ ) state, and

$$\gamma(^3P_1) = 9.0 \times 10^3 P_{\text{Ne}} \quad (20)$$

for Ne( $^3P_1$ ) atoms. The quantities  $\gamma(^1P_1)$  and  $\gamma(^3P_1)$  are in units of  $\text{sec}^{-1}$ . The two-body coefficient in Eq. (20) represents the final decay of the Ne( $^3P_1$ ) level. Note that for all the measurements reported in this section  $P_{\text{He}} \gg P_{\text{Ne}}$ . Therefore, at each constant helium pressure, the collision coefficients given by Eqs. (19) and (20) represent destruction rates for Ne( $^1P_1$ ) and Ne( $^3P_1$ ) atoms in collisions with helium ground-state atoms.

The above results give no information about the many important transitions in the visible and infrared regions of the spectrum. In the interpretation of the measured decay rates, we therefore rely strongly on gas-discharge investigations of energy transfers in He-Ne mixtures. Transfer of excitation from He( $2^1S$ ) to neon presents a number of possibilities. The 3s, 4s, 5s, 3d, 4d, and 5d neon levels (in Paschen notation) all lie within about  $10^{-2}$  eV of He( $2^1S$ ). However, experimental evidence (see, e.g., Refs. 12 and 21) appears to indicate that energy transfer from He( $2^1S$ ) is primarily to Ne( $3s_2$ ), the upper level of the 6328-Å laser transition. Thus, Massey *et al.*<sup>12</sup> have found that the total destruction cross section ( $Q \approx 4.1 \times 10^{-16} \text{ cm}^2$ ) for He( $2^1S$ ) is consistent with the reaction



The forward resonant-transfer rate coefficient for this reaction can be calculated from the total destruction cross section for He( $2^1S$ ) and is given by<sup>13</sup>

$$k_r \approx 2.4 \times 10^6 \text{ sec}^{-1}/\text{Torr} \quad (22)$$

An important kinetic process at helium pressures of a few hundred Torr and above is the reverse

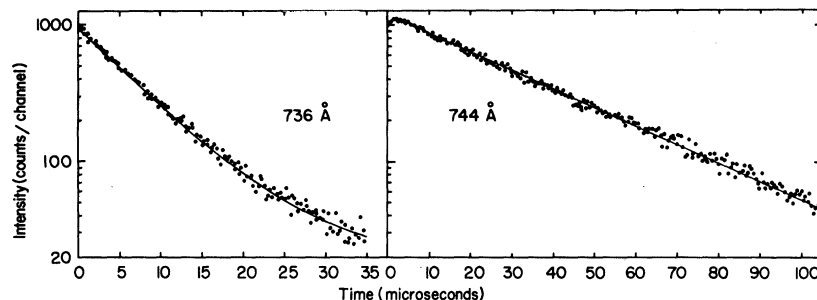


FIG. 10. Time-resolved spectra of the emissions from Ne( $^1P_1$ ) and Ne( $^3P_1$ ) in 200 Torr of helium and 0.06 Torr of neon.

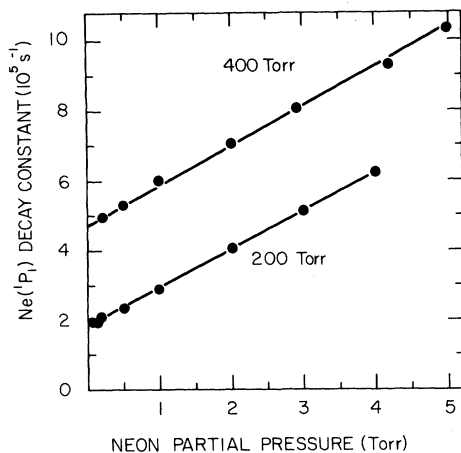
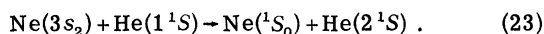


FIG. 11.  $\text{Ne}(^1P_1)$  decay constant at helium pressures of 200 and 400 Torr as a function of neon partial pressure.

resonant-transfer reaction



The reverse-transfer rate coefficient may be obtained from considerations of detailed balancing<sup>10</sup> and at 300 K has been calculated to be<sup>13</sup>

$$k'_r \approx 9.4 \times 10^6 \text{ sec}^{-1}/\text{Torr}. \quad (24)$$

For the helium pressures used in this experiment, the reverse-transfer rate exceeds the forward-transfer rate and the inverse lifetime ( $A \approx 1.3 \times 10^7 \text{ sec}^{-1}$ ) of the  $\text{Ne}(3s_2)$  level by several orders of magnitude. Furthermore, at these relatively high helium pressures, collisional deexcitation of  $\text{Ne}(3s_2)$  to other nearby neon levels must be taken into consideration. Energy transfer from  $\text{He}(2^1S)$  and from  $\text{Ne}(3s_2)$  to the  $3s_{3,4,5}$  levels of neon violates the Wigner spin rules, as discussed by Bennett.<sup>22</sup> Massey *et al.* have estimated maximum cross sections for energy-transfer processes which do not comply with the Wigner spin rules. Their estimates are based on ratios of calculated  $A$  coefficients and on measured relative populations. The results are:

$$Q_{\max} [\text{He}(2^1S) + \text{Ne}(1^1S_0) \rightarrow \text{He}(1^1S) + \text{Ne}(3s_{3,4,5})] \leq 10^{-18} \text{ cm}^2, \quad (25)$$

$$Q_{\max} [\text{Ne}(3s_2) + \text{He}(1^1S) \rightarrow \text{Ne}(3s_{3,4,5}) + \text{He}(1^1S)] \leq 4 \times 10^{-17} \text{ cm}^2. \quad (26)$$

Note that the cross section (25) is two orders of magnitude smaller than the total destruction cross section for  $\text{He}(2^1S)$ . At low neon pressures, this process may therefore be neglected. On the other hand, Eq. (26) shows that collisional excitation transfer from  $\text{Ne}(3s_2)$  should play an impor-

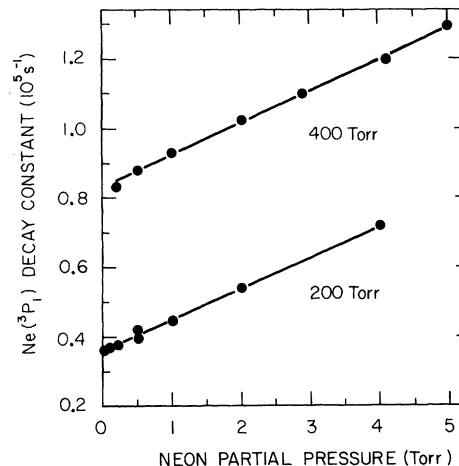


FIG. 12.  $\text{Ne}(^3P_1)$  decay constant at helium pressures of 200 and 400 Torr as a function of neon partial pressure.

tant role in a high-pressure helium host gas. Because of the large reverse-transfer rate, the net destruction frequency of  $\text{He}(2^1S)$  depends strongly on the rate at which excitation can be transferred from  $\text{Ne}(3s_2)$  to other neon levels. One would therefore expect the two-body collision coefficient for  $\text{He}(2^1S)$  to be dependent upon such energy transfers. Furthermore, the lowest-lying neon states are populated by cascading, so that their pressure dependence is coupled to the pressure dependence of the  $\text{Ne}(3s_2)$  population.

These excitation-transfer processes are depicted in Fig. 13 with the collision coefficient  $k$  as the only unknown. The rate equations governing energy transfer may be written as

$$\frac{dM_2}{dt} = -k_r P_{\text{Ne}} M_2 + k'_r P_{\text{He}} R_2, \quad (27)$$

$$\frac{dR_2}{dt} = k_r P_{\text{Ne}} M_2 - [(k'_r + k) P_{\text{He}} + A] R_2, \quad (28)$$

where  $M_2$  and  $R_2$  denote the number of  $\text{He}(2^1S)$  and  $\text{Ne}(3s_2)$  atoms, respectively. The quantity  $A$  represents spontaneous emission. The solution of the coupled differential equations is of the form

$$R_2(t) = B_1 e^{-\lambda_1 t} + B_2 e^{-\lambda_2 t}, \quad (29)$$

where  $B_1$  and  $B_2$  are constants. In Appendix B it is shown that for  $P_{\text{He}} \gg P_{\text{Ne}}$  the decay constants  $\lambda_1$  and  $\lambda_2$  may be approximated by

$$\lambda_1 \approx (k'_r + k) P_{\text{He}} + k_r P_{\text{Ne}} + A, \quad (30)$$

$$\lambda_2 \approx (k P_{\text{He}} + A) k_r P_{\text{Ne}} [(k'_r + k) P_{\text{He}} + k_r P_{\text{Ne}} + A]^{-1}. \quad (31)$$

At sufficiently low gas pressures, radiative processes are dominant, so that  $\lambda_1 \approx A$  and  $\lambda_2 \approx k_r P_{\text{Ne}}$ .

Under these conditions the two terms in Eq. (29) represent radiative deexcitation and collisional excitation of  $\text{Ne}(3s_2)$  atoms, respectively.

As helium pressure is increased, collisional processes provide the dominant decay mechanism. From the reverse-transfer rate (24) and the cross-section estimate (26) it follows that  $k'_r \gg k$ . Furthermore, for the helium pressures used in this work we have  $k'_r P_{\text{He}} \gg k_r P_{\text{Ne}}$ ,  $A$ . The decay constants then simplify to

$$\lambda_1 \approx k'_r P_{\text{He}} \quad (30')$$

$$\lambda_2 \approx (k P_{\text{He}} + A) k_r P_{\text{Ne}} / k'_r P_{\text{He}} \quad (31')$$

At high helium pressures,  $\lambda_1$  represents primarily the reverse excitation transfer from  $\text{Ne}(3s_2)$  to  $\text{He}(2^1S)$ . Furthermore, Eqs. (31) and (31') show that as helium pressure is increased to a few hundred Torr, the magnitude of  $\lambda_2$  decreases because of the reverse-transfer rate  $k'_r P_{\text{He}}$ . If the helium density is sufficiently high so that  $k P_{\text{He}} \gg A$ ,  $\lambda_2$  becomes independent of helium pressure, and we have

$$\lambda_2 \approx k(k_r/k'_r) P_{\text{Ne}} \quad (31'')$$

The experimental data indicate that the last equation is valid for the helium pressures used in this work.

The collision coefficient  $k$  can be determined from the time dependence of the  $\text{Ne}(^1P_1)$  emissions. This assumes that lower-lying neon levels, in particular the  $\text{Ne}(2p)$  states, decay primarily by radiative processes, so that no new pressure dependencies are introduced at these levels. The data of Soldatov *et al.*<sup>15</sup> indicate that, for low neon partial pressures, the population of the lowest excited states is determined by cascading from the  $\text{Ne}(2p)$  levels. It is also assumed that the decay of  $\text{Ne}(^1P_1)$  atoms in helium is fast, so that excitation transfer from the  $\text{Ne}(3s_2)$  level is the rate-limiting step. Based on these assumptions, we should have  $\lambda_2$

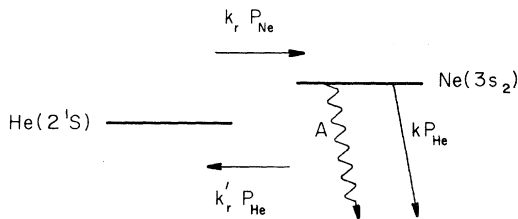


FIG. 13. Rate diagram for excitation transfer in He-Ne mixtures. Symbols used:  $k_r$ —forward resonant transfer,  $k'_r$ —reverse resonant transfer,  $A$ —spontaneous emission,  $k$ —collisional deexcitation of  $\text{Ne}(3s_2)$  atoms to other neon levels.

$\approx \gamma(^1P_1)$ . From Eqs. (19) and (31'') we find

$$k \approx 4.3 \times 10^5 \text{ sec}^{-1}/\text{Torr} \quad (32)$$

This is in good agreement with the measured two-body collision coefficient (18) for the destruction of  $\text{He}(2^1S)$  atoms. The result shows that in a high-pressure helium host gas the net rate of excitation transfer from  $\text{He}(2^1S)$  to  $\text{Ne}(3s_2)$  is governed by the rate at which energy is collisionally transferred from  $\text{Ne}(3s_2)$  to other neon levels. Furthermore, it is seen from Eq. (31'') that the decay constant  $\lambda_2$  contains the ratio  $k_r/k'_r$ , so that the observable decay of  $\text{Ne}(3s_2)$  is reduced from  $k P_{\text{Ne}}$  by this ratio. It is the quantity  $k(k_r/k'_r) P_{\text{Ne}}$  that is measured at the wavelength of the resonance state  $\text{Ne}(^1P_1)$ .

The two-body collision coefficient  $k$  given by Eq. (32) corresponds to a velocity-averaged cross section of about  $8 \times 10^{-17} \text{ cm}^2$ . This is twice the value of the cross-section estimate (26). It may reflect an inaccuracy in the estimate. On the other hand, the rate constant  $k$  represents the total destruction rate of  $\text{Ne}(3s_2)$  atoms in collisions with helium ground-state atoms. It may include excitation transfer to levels other than the  $3s$  levels. If such processes play an important role, one would expect the total destruction cross section to be greater than indicated by Eq. (26). Afterglow experiments<sup>14,23</sup> appear to indicate that energy may be transferred from  $\text{Ne}(3s_2)$  to a number of levels other than the  $3s$  levels. Further discussion of this problem is given in Sec. V.

Finally, we analyze the emissions from the resonance state  $\text{Ne}(^3P_1)$ . The data of Soldatov *et al.* show that the lowest excited states of neon are populated primarily by cascading from the  $\text{Ne}(2p)$  levels. Furthermore, the populations of  $\text{Ne}(^3P_1)$  and  $\text{Ne}(^3P_2)$  were found to be nearly equal and considerably larger than those of  $\text{Ne}(^1P_1)$  and  $\text{Ne}(^3P_0)$ . As in the case of pure neon, the time dependence of the emissions from  $\text{Ne}(^3P_1)$  reflects collisional deexcitation to the lowest metastable state. It has been shown by Phelps that two-body collision coefficients in mixtures may be determined from a linear superposition of these processes in the pure gases. Thus,

$$k_{\text{He-Ne}} = (k_{\text{He}} P_{\text{He}} + k_{\text{Ne}} P_{\text{Ne}}) / (P_{\text{He}} + P_{\text{Ne}}) \quad (33)$$

where  $k_{\text{He-Ne}}$  is the coefficient for the mixture, and  $k_{\text{He}}$  and  $k_{\text{Ne}}$  are the coefficients for the pure gases helium and neon, respectively. In the experiment reported here,  $P_{\text{He}} \gg P_{\text{Ne}}$ , so that  $k_{\text{He-Ne}} \approx k_{\text{He}}$ . This expresses the fact that, since  $P_{\text{He}} \gg P_{\text{Ne}}$ ,  $\text{Ne}(^3P_1)$  atoms are destroyed primarily in collisions with helium ground-state atoms. When measured as a function of neon partial pressure, the quantity observed is  $k_{\text{He}} P_{\text{Ne}}$ .

The two-body collision coefficient for the  $\text{Ne}(^3P_2)$ -to- $\text{Ne}(^3P_1)$  transition in helium given by Phelps is about  $6.7 \times 10^3 \text{ sec}^{-1} \text{ Torr}$ . At helium pressures of a few hundred Torr a large fraction of  $\text{Ne}(^3P_2)$  atoms is therefore rapidly excited to the  $\text{Ne}(^3P_1)$  level. This collisional excitation presumably contributes to the initial buildup in intensity of the emissions from  $\text{Ne}(^3P_1)$ . From detailed balancing,<sup>4</sup> it follows that the deexcitation rate from  $\text{Ne}(^3P_1)$  to  $\text{Ne}(^3P_2)$  is about 12.4 times as large as the excitation rate. Therefore, in the mixture,  $\text{Ne}(^3P_1)$  atoms should be destroyed at the rate of about  $8.3 \times 10^3 \text{ sec}^{-1} / \text{Torr}$ . Rate equations similar to those used in Appendix A, with the omission of three-body terms, may be used to analyze  $\text{Ne}(^3P_1)$  decay in helium. It is easily shown [see Eq. (A10)] that the observed collisional deexcitation corresponds to the sum of the coefficients  $k_{\text{He-Ne}}(^3P_1 \rightarrow ^3P_2) + k_{\text{He-Ne}}(^3P_2 \rightarrow ^3P_1)$ . Based on detailed balancing, this is about  $9 \times 10^3 \text{ sec}^{-1} / \text{Torr}$ , in excellent agreement with the measured value given by Eq. (20).

#### V. SUMMARY AND DISCUSSION

The analysis of experimental data for neon has shown that, at low pressures, atoms in the  $\text{Ne}(^1P_1)$  state are destroyed by the escape of resonance radiation and by collisional deexcitation to the  $\text{Ne}(^3P_1)$  level. The latter conclusion was based on the time evolution of the emissions from the two resonance states and on potential-energy curve crossings. Atoms in the  $\text{Ne}(^3P_1)$  level are deexcited by the escape of resonance radiation, by collision-induced transition to  $\text{Ne}(^3P_2)$ , and by three-body collisions involving two neon ground-state atoms. Metastable  $\text{Ne}(^3P_2)$  atoms are depleted by collisional excitation to the  $\text{Ne}(^3P_1)$  level and by three-body collisions. The two-body coefficient for  $\text{Ne}(^3P_1)$  and two- and three-body collision coefficients for  $\text{Ne}(^3P_2)$  were found to be in good agreement with the results of Phelps. Based upon measured decay rates, a model was constructed for the formation of excited neon molecules. This model is consistent with theory.<sup>5,6</sup> The three-body destruction rate of  $\text{Ne}(^3P_2)$  atoms is in quantitative agreement with the time evolution of the neon continuum emissions reported previously.<sup>3</sup>

Measurements of the vacuum-uv emissions from He-Ne mixtures indicate that excited helium molecules play no role in the excitation of the lowest excited states of neon. The analysis of time-resolved data has shown that some of the excitation energy of the  $\text{He}(2^1S)$  metastable is ultimately deposited in the  $\text{Ne}(^1P_1)$  and  $\text{Ne}(^3P_{0,1,2})$  levels. Measured decay constants for  $\text{He}(2^1S)$  and  $\text{Ne}(^1P_1)$

atoms are consistent with gas-discharge results<sup>9,12,13</sup> for excitation transfer from  $\text{He}(2^1S)$  to the  $\text{Ne}(3s_2)$  laser level. However, more information about energy transfers from  $\text{Ne}(3s_2)$  to other neon levels would be desirable. The data analysis indicates that the destruction cross section for  $\text{Ne}(3s_2)$  may be twice as large as previously estimated. This analysis was based on the assumption that the pressure dependence of lower neon levels, for example the  $2p$  states, follows the pressure dependence of the  $\text{Ne}(3s_2)$  level. If these lower levels are also collisionally excited or deexcited so that new pressure dependencies are introduced, the calculated value for the destruction of  $\text{Ne}(3s_2)$  atoms would be in error. A further possibility is that excitation is transferred from  $\text{Ne}(3s_2)$  to levels other than the  $\text{Ne}(3s_{3,4,5})$  states. In this case, the total destruction cross section for  $\text{Ne}(3s_2)$  should be greater than estimated by Massey *et al.*<sup>12</sup> At present, there appear to be no time-resolved studies to answer these questions. Nevertheless, the two-body collision coefficient for  $\text{Ne}(3s_2)$  atoms appears to be of the right order of magnitude.

The experiment reported here gives no experimental input about the triplet states of helium. The rate equations for excitation transfer in He-Ne mixtures are based on the experimental observation<sup>13</sup> that the  $\text{He}(2^1S)$  level is decoupled from the  $\text{He}(2^3S)$  level. Furthermore, the low excitation currents used in this experiment make transitions between singlet and triplet populations much less important than is the case in gas-discharge studies. The triplet states should have almost no effect on the emissions.

Tables I and II summarize the reactions and rate constants investigated in this work.

#### ACKNOWLEDGMENTS

We are grateful to M. G. Payne, G. S. Hurst, and R. E. Knight for many informative discussions.

#### APPENDIX A: DECAY CONSTANTS FOR $\text{Ne}(^3P_1)$ AND $\text{Ne}(^3P_2)$

The rate equations (7) and (8) may be written as

$$(D + \beta_2 + k_2 P_{\text{Ne}} + k_3 P_{\text{Ne}}^2) R_1 = k_4 P_{\text{Ne}} M_1, \quad (\text{A1})$$

$$(D + k_4 P_{\text{Ne}} + k_5 P_{\text{Ne}}^2) M_1 = k_2 P_{\text{Ne}} R_1, \quad (\text{A2})$$

where  $D = d/dt$ . The collision coefficients  $k_2$  to  $k_5$  will be evaluated in terms of the experimentally determined decay constants

$$\tau_1 = 1.86 \times 10^4 + 1.80 \times 10^3 P_{\text{Ne}} + 5.18 P_{\text{Ne}}^2,$$

$$\tau_2 = 160 P_{\text{Ne}} + 0.40 P_{\text{Ne}}^2.$$

The simultaneous equations (A1) and (A2) lead to

TABLE I. Measured two- and three-body rate constants in neon (two-body rates in  $\text{sec}^{-1}/\text{Torr}$ , three-body rates in  $\text{sec}^{-1}/\text{Torr}^2$ ).

Reaction	Rate Constant
$\text{Ne}(^1P_1) + \text{Ne}(^1S_0) \rightarrow \text{Ne}(^3P_1) + \text{Ne}(^1S_0)$	$5.5 \times 10^4$
$\text{Ne}(^3P_1) + \text{Ne}(^1S_0) \rightarrow \text{Ne}(^3P_2) + \text{Ne}(^1S_0)$	$1.8 \times 10^3$
$\text{Ne}(^3P_2) + \text{Ne}(^1S_0) \rightarrow \text{Ne}(^3P_1) + \text{Ne}(^1S_0)$	$1.6 \times 10^2$
$\text{Ne}(^3P_1) + 2\text{Ne}(^1S_0) \rightarrow \text{Ne}_2(0_u^+) + \text{Ne}(^1S_0)$	5.0
$\text{Ne}(^3P_2) + 2\text{Ne}(^1S_0) \rightarrow \text{Ne}_2(1_u) + \text{Ne}(^1S_0)$	0.60

$$(D^2 + a_1 D + b_1)R_1 = 0, \quad (\text{A3})$$

with

$$a_1 = \beta_2 + (k_2 + k_4)P_{\text{Ne}} + (k_3 + k_5)P_{\text{Ne}}^2, \quad (\text{A4})$$

$$b_1 = \beta_2(k_4 + k_5 P_{\text{Ne}})P_{\text{Ne}} + [k_3 k_4 + k_5(k_2 + k_3 P_{\text{Ne}})]P_{\text{Ne}}^3. \quad (\text{A5})$$

The solution of Eq. (A3) is

$$R_1(t) = A_1 e^{-r_1 t} + A_2 e^{-r_2 t}, \quad (\text{A6})$$

where  $A_1$  and  $A_2$  are constants, and where

$$r_{1,2} = \frac{1}{2}a_1 [1 \mp (1 - 4b_1/a_1^2)^{1/2}], \quad (\text{A7})$$

so that

$$a_1 = r_1 + r_2, \quad (\text{A8})$$

$$b_1 = r_1 r_2. \quad (\text{A9})$$

The number of unknowns in Eqs. (A4) and (A5) may be reduced by first considering the low-pressure region. At sufficiently low neon pressures, the three-body terms may be neglected, and we have

$$a_1 \approx \beta_2 + (k_2 + k_4)P_{\text{Ne}}. \quad (\text{A10})$$

From (A8) and (A10) it follows that

$$k_2 + k_4 = (r'_1 + r'_2 - \beta_2)/P_{\text{Ne}} = 1.96 \times 10^3 \quad (\text{A11})$$

in units of  $\text{sec}^{-1}/\text{Torr}$ . The quantities  $r'_1$  and  $r'_2$  include only the terms that are linear in pressure and the constant  $\beta_2$  of the experimental values of  $r_1$  and  $r_2$ . Next, we use Eq. (A9) and keep only linear pressure terms in the product  $r_1 r_2$ . That is,

$$r_1 r_2 \approx \beta_2 k_4 P_{\text{Ne}} = (1.84 \times 10^4) 160 P_{\text{Ne}}. \quad (\text{A12})$$

From the last two equations we obtain  $k_2 \approx 1.8 \times 10^3 \text{ sec}^{-1}/\text{Torr}$  and  $k_4 \approx 160 \text{ sec}^{-1}/\text{Torr}$ . Note that  $k_2/k_4 \approx 11.3$ , in reasonable agreement with the value of 12.4 based on detailed balancing.<sup>4</sup> An alternate procedure for finding  $k_2$  and  $k_4$  is to apply detailed balancing and to use the relation

TABLE II. Measured rate constants in high-pressure He-Ne mixtures.

Reaction	Rate Constant ( $\text{sec}^{-1}/\text{Torr}$ )
$\text{He}(2'S) + \text{Ne}(^1S_0) \rightarrow \text{Ne}(^3S_2) + \text{He}(1'S)$	$4.1 \times 10^5$
$\text{Ne}(^1P_1) + \text{He}(1'S) \rightarrow \text{Ne}(^3P_1) + \text{He}(1'S)$	$1.1 \times 10^5$
$\text{Ne}(^3P_1) + \text{He}(1'S) \rightarrow \text{Ne}(^3P_2) + \text{He}(1'S)$	$8.3 \times 10^3$

$k_2 \approx 12.4 k_4$  in Eq. (A11). Within experimental error, this yields the same results. The above values of  $k_2$  and  $k_4$  are in good agreement with the measurements of Phelps.

For pressures of the order of 1000 Torr, Eqs. (A4) and (A5) may be approximated by

$$a_1 \approx (k_2 + k_4)P_{\text{Ne}} + (k_3 + k_5)P_{\text{Ne}}^2, \quad (\text{A13})$$

$$b_1 \approx [k_3 k_4 + k_5(k_2 + k_3 P_{\text{Ne}})]P_{\text{Ne}}^3. \quad (\text{A14})$$

Using (A8) and (A13), one has

$$k_3 + k_5 = [r_1 + r_2 - (k_2 + k_4)P_{\text{Ne}}]/P_{\text{Ne}}^2,$$

where  $r_1$  and  $r_2$  now include the full pressure dependence. Pressure is assumed to be high enough so that  $\beta_2$  is negligible compared with the pressure-dependent terms of  $r_1$ . Then

$$k_3 + k_5 = 5.58, \quad (\text{A15})$$

in units of  $\text{sec}^{-1}/\text{Torr}^2$ . The coefficients  $k_3$  and  $k_5$  can be found by solving Eqs. (A9) and (A15) with  $b_1$  given by (A14). This results in  $k_3 \approx 5.0 \text{ sec}^{-1}/\text{Torr}^2$  and  $k_5 \approx 0.60 \text{ sec}^{-1}/\text{Torr}^2$ . The three-body coefficient  $k_5$  is in good agreement with the value obtained by Phelps.

#### APPENDIX B: DECAY CONSTANTS FOR $\text{He}(2^1S)$ TO $\text{Ne}(3s_2)$ EXCITATION TRANSFER

To find a solution of the coupled differential equations (28) and (29), we write

$$(D + k_r P_{\text{Ne}})M_2 = k'_r P_{\text{He}} R_2, \quad (\text{B1})$$

$$[D + (k'_r + k)P_{\text{He}} + A]R_2 = k_r P_{\text{Ne}} M_2, \quad (\text{B2})$$

where  $D = d/dt$ ,  $k_r \approx 2.4 \times 10^6$ ,  $k'_r \approx 9.4 \times 10^6$  in units of  $\text{sec}^{-1}/\text{Torr}$ . The quantity  $A$  is about  $1.3 \times 10^7 \text{ sec}^{-1}$ . Solving Eqs. (B1) and (B2) in terms of  $R_2$ , we find

$$(D^2 + a_2 D + b_2)R_2 = 0, \quad (\text{B3})$$

with

$$a_2 = (k'_r + k)P_{\text{He}} + k_r P_{\text{Ne}} + A, \quad (\text{B4})$$

$$b_2 = (k P_{\text{He}} + A)k_r P_{\text{Ne}}. \quad (\text{B5})$$

Equation (B3) has the solution

$$R_2(t) = B_1 e^{-\lambda_1 t} + B_2 e^{-\lambda_2 t},$$

where

$$\lambda_{1,2} = \frac{1}{2} a_2 [1 \mp (1 - 4b_2/a_2^2)^{1/2}]. \quad (\text{B6})$$

As explained in the text,  $k' \gg k$ . For He-Ne mixtures which satisfy  $P_{\text{He}} \gg P_{\text{Ne}}$ , we have  $a_2^2 \gg b_2$  for sufficiently low and sufficiently high gas pres-

ures. The square root in Eq. (B6) may therefore be expanded with the result

$$\lambda_1 \approx a_2, \quad (\text{B7})$$

$$\lambda_2 \approx b_2/a_2. \quad (\text{B8})$$

Substitution of Eqs. (B4) and (B5) in the last two equations leads immediately to Eqs. (30) and (31) given in the text.

- 
- <sup>1</sup>See, for example, H. A. Koehler, L. J. Ferderber, D. L. Redhead, and P. J. Ebert, *Appl. Phys. Lett.* **21**, 198 (1972); P. W. Hoff, J. C. Swingle, and C. K. Rhodes, *Opt. Commun.* **3**, 128 (1973); J. B. Gerardo and A. W. Johnson, *IEEE J. Quantum Electron.* **QE-9**, 748 (1973); W. M. Hughes, J. Shannon, A. Kolb, E. Ault, and M. Bhaumik, *Appl. Phys. Lett.* **23**, 385 (1973).
- <sup>2</sup>D. C. Lorents and R. E. Olsen, Stanford Research Institute, Final Report, 1973 (unpublished).
- <sup>3</sup>P. K. Leichner, *Phys. Rev. A* **8**, 815 (1973).
- <sup>4</sup>A. V. Phelps, *Phys. Rev.* **114**, 1011 (1959).
- <sup>5</sup>J. S. Cohen and B. I. Schneider, *J. Chem. Phys.* **61**, 3230 (1974).
- <sup>6</sup>B. I. Schneider and J. S. Cohen, *J. Chem. Phys.* **61**, 3240 (1974).
- <sup>7</sup>D. M. Bartell, G. S. Hurst, and E. B. Wagner, *Phys. Rev. A* **7**, 1068 (1973).
- <sup>8</sup>J. R. Dixon and F. A. Grant, *Phys. Rev.* **107**, 118 (1957).
- <sup>9</sup>E. E. Benton, E. E. Ferguson, F. A. Matsen, and W. W. Robertson, *Phys. Rev.* **128**, 206 (1962).
- <sup>10</sup>A. D. White and E. I. Gordon, *Appl. Phys. Lett.* **3**, 197 (1963).
- <sup>11</sup>A. Javan, W. R. Bennett, and D. R. Herriott, *Phys. Rev. Lett.* **6**, 106 (1961).
- <sup>12</sup>J. T. Massey, A. G. Schulz, B. F. Hochheimer, and S. M. Cannon, *J. Appl. Phys.* **36**, 658 (1965).
- <sup>13</sup>R. Arrathoon, *J. Appl. Phys.* **40**, 2875 (1965).
- <sup>14</sup>R. Arrathoon, *Phys. Rev. A* **4**, 203 (1971).
- <sup>15</sup>A. N. Soldatov, G. S. Evtushenko, and I. I. Muravev, *Opt. Spetrosk.* **34**, 13 (1973) [*Opt. Spectrosc.* **34**, 6 (1973)].
- <sup>16</sup>T. Holstein, *Phys. Rev.* **72**, 1212 (1947); **83**, 1159 (1951).
- <sup>17</sup>G. M. Lawrence and H. S. Liszt, *Phys. Rev.* **178**, 122 (1969).
- <sup>18</sup>M. G. Payne, J. E. Talmadge, G. S. Hurst, and E. B. Wagner, *Phys. Rev. A* **9**, 1050 (1974).
- <sup>19</sup>M. G. Payne, C. E. Klots, and G. S. Hurst (unpublished).
- <sup>20</sup>A. Gedanken, J. Jortner, B. Raz, and A. Szoke, *J. Chem. Phys.* **57**, 3456 (1972).
- <sup>21</sup>A. D. White and J. D. Rigden, *Proc. IRE* **50**, 1697 (1972).
- <sup>22</sup>W. R. Bennett, Jr., *Appl. Opt. Suppl.* **1**, 24 (1962).
- <sup>23</sup>R. A. McFarlane, W. L. Faust, and C. K. N. Patel, *Proc. IEEE* **51**, 468 (1963).